Dynamic Gap Junctional Communication: A Delimiting Model for Tissue Responses

G. J. Christ,* P. R. Brink,‡ and S. V. Ramanan‡

*Department of Urology, Albert Einstein College of Medicine, Bronx, New York 10461, and ‡Department of Physiology and Biophysics, State University of New York at Stony Brook, Stony Brook, New York 11794 USA

ABSTRACT Gap junctions are aqueous intercellular channels formed by a diverse class of membrane-spanning proteins, known as connexins. These aqueous pores provide partial cytoplasmic continuity between cells in most tissues, and are freely permeable to a host of physiologically relevant second messenger molecules/ionic species (e.g., Ca^{2+}, IP3, cAMP, cGMP). Despite the fact that these second messenger molecules/ionic species have been shown to alter junctional patency, there is no clear basis for understanding how dynamic and transient changes in the intracellular concentration of second messenger molecules might modulate the extent of intercellular communication among coupled cells. Thus, we have modified the tissue monolayer model of Ramanan and Brink (1990) to account for both the up-regulatory and down-regulatory effects on junctions by second messenger molecules that diffuse through gap junctions. We have chosen the vascular wall as our morphological correlate because of its anisotropy and large investment of gap junctions. The model allows us to illustrate the putative behavior of gap junctions under a variety of physiologically relevant conditions. The modeling studies demonstrated that transient alterations in intracellular second messenger concentrations are capable of producing 50–125% changes in the number of cells recruited into a functional syncytial unit, after activation of a single cell. Moreover, the model conditions required to demonstrate such physiologically relevant changes in intercellular diffusion among coupled cells are commonly observed in intact tissues and cultured cells.

INTRODUCTION

Gap junctions are aqueous intercellular channels formed by a diverse class of membrane-spanning proteins, known as connexins (Hall et al., 1993). These aqueous pores permit the rapid intercellular transit of ions and small molecules up to a molecular mass of 1000 daltons. Their ubiquitous distribution throughout the body and generally permissive nature have led many investigators to propose that gap junctions play an active role in normal tissue homeostasis, as well as the etiology of a variety of diseases (Hall et al., 1993). For example, gap junctions have been demonstrated to play an obligatory role in synchronizing contraction of ventricular myocardium (Barr et al., 1965; Spray and Burt, 1990; Brink, 1991; Spray et al., 1993) and myometrial smooth muscle contractions at parturition (Cole et al., 1985; Daniel, 1987; Risek et al., 1990), as well as coordinating vasomotor responses (Christ et al., 1993a, 1993b; Spray et al., 1993; Moore et al., 1991; Segal and Duling, 1986; Larson et al., 1990). In addition, they are known to be involved in the delineation of communication compartments during normal embryonic development (Sheridan, 1987; Egbahli et al., 1991; Minkoff et al., 1993) and perhaps the coordination of pancreatic secretions (Kanno et al., 1993; Chanson and Meda, 1993). Moreover, altered junctional communication has been hypothesized to be a significant etiologic factor in

a host of disease processes, ranging from cardiac arrhythmias (Spray et al., 1993; Brink, 1991; Spear et al., 1990a, 1990b) to cancer (Kanno, 1985; Yamasaki, 1987; Trosko, 1990a, 1990b; Egbahli et al., 1991) and vascular dysfunction (Christ et al., 1993a, 1993b; Spray et al., 1993; Moore et al., 1991; Segal and Duling, 1986; Larson et al., 1990).

Unfortunately, it has not been illustrated how changes in the extent of intercellular communication among coupled cells might participate in modulating tissue homeostasis and/or be involved in the pathogenesis of disease. Both possibilities warrant serious consideration, because a dynamic role for gap junctions in the modulation of tissue responses has been suggested by two important experimental observations: 1) the demonstration of the rapid intercellular transit of physiologically relevant receptor-activated second messenger molecules through gap junctions between coupled cells (Tsien and Weingart, 1976; Saez et al., 1989; Sanderson et al., 1990; Christ et al., 1992; Cornell-Bell et al., 1990), and 2) junctional permeability/conductance has been shown to be regulated by those same second messenger molecules to which the channels are freely permeable (De Mello, 1988; Moore et al., 1991; Takens-kwak and Jongsma, 1992; Moreno et al., 1992, 1993). The former observation demonstrates that gap junctions provide an important conduit for coordination of tissue responses. The latter observation demonstrates that changes in second messenger formation/stimulation can have a significant impact on the degree of intercellular communication.

In an attempt to determine the role of gap junctions in tissues, we have developed a diffusion-based model that illustrates how dynamic changes in junctional membrane patency might affect intercellular messenger driven processes. Moreover, the model provides a framework for producing

experimentally testable hypotheses concerning the manifold roles of gap junctions in tissue function and disease.

MATERIALS AND METHODS

Assumptions

The model that is developed here is similar to the one-dimensional model treated in Ramanan and Brink (1990). A linear chain of cells, each of width $2a$, are coupled together by junctional membranes. Diffusion inside the cells obeys Fick's law, embodied in the diffusion coefficient D. The permeability of the junctional membrane is represented by a permeability coefficient P. Ramanan and Brink (1990) regarded the permeability coefficient P as a fixed quantity; the diffusing substance did not have any modulatory effects on the (gap junction) channels that are presumably the physical mechanism underlying P. In studying the diffusion of substances that do modulate the open probability of gap junction channels (for instance), the assumption of a fixed permeability P will no longer hold. In the model presented here, we allow the permeability coefficient P to depend dynamically on the concentrations of the diffusing substance within the two abutting cells that make the membrane interface.

The main assumption in the foregoing is that gap junction-mediated diffusion between cells can be modeled as a one-dimensional process. Many tissues that contain cells linked by gap junctions are anisotropic with regard to cell length and width. For example, cardiac and various smooth muscles fit this criterion. Gap junctions are often found all along the surface of such cell types; an example is the arteriolar wall. There the smooth muscle cells have gap junctions all along their lateral borders (Christ et al., 1993, Fig. 6). There are then two distinguishing features about the geometry of the cells that we are modeling: (1) they are long and thin, lying roughly parallel along their lengths; (2) the abutting long surfaces are rich, and uniformly so, in gap junctions. In addition, it has been well established that neuronal innervation of the vascular wall is confined to the adventitial-medial smooth muscle border (Hirst and Edwards, 1987; Gibbins et al., 1988). Although the exact innervation density has not been established and can vary among distinct blood vessels (with more intimate innervation characteristic of the smaller blood vessels), we are assuming that the innervation of most blood vessels is sufficient (i.e., 1:1, 1:3) to permit relatively homogeneous and simultaneous activation of the outer layer of vascular smooth muscle cells.

We also assume that the diffusing substance *uniformly* fills the injected outer layer at the initial time, and that there is no production of the substance

thereafter. We are then assuming that, after cellular activation, there is a rapid and transient increase (impulse) in an intracellular second messenger concentration to some peak value. An example can be found in the receptor-activated Ca^{2+} transients visualized using Fura-2 techniques in many cell types.

Under such conditions, the concentration of the diffusing substance at all times is uniform over the cell length (≈ 100 μm) and the diffusion paths and, hence, the concentration gradients, are across the cell width (≈ 10 μm). Hence, diffusion out of the primary layer (most intimate with the innervation source) can be modeled as a one-dimensional process into the depths of the tissue. The primary outer injected layer is replaced by a single cell homogenously injected with messenger at time $t = 0$ with concentration C_{inj}. Each sheet of noninnervated cells below the adventitial-medial layer is represented in the one-dimensional model by a single cell (see Fig. 1); these cells have zero concentration of messenger at time $t = 0$.

The model

For the diffusion inside the ith cell ($i \geq 0$), we have

$$D \frac{\partial^2 C}{\partial x^2} = \frac{\partial C}{\partial t} \qquad 2ia < x < 2(i + 1)a. \tag{1}$$

At the boundary between the ith cell and the $(i + 1)$th cell,

$$D \frac{\partial C}{\partial x} = P(C^+ - C^-) \qquad x = 2ia \tag{2}$$

Here $C^+ = C(x^+)$ and $C^- = C(x^-)$ are the concentrations at the edges x^+ and x^- of the two cells that constitute the interface. As noted above, the permeability P will itself be a function of C^+ and C^-. At the boundary $x = 0$ of the injected cell ($i = 0$), there is no flux across the boundary, i.e.,

$$\left| \frac{\partial C}{\partial x} \right|_{x=0} = 0 \tag{3}$$

We assume that the permeability P is solely because of gap junction channels. Hence, here and hereafter, we use the term "channel" to mean "gap junction channel." To isolate the effects of modulation on P, we decompose P as $P = Np\wp$, where N is the number of (active) channels in the interface (assumed to be the same for all interfaces), $\wp$ is the intrinsic permeability of the channel to the diffusing substance, and p is the open probability of
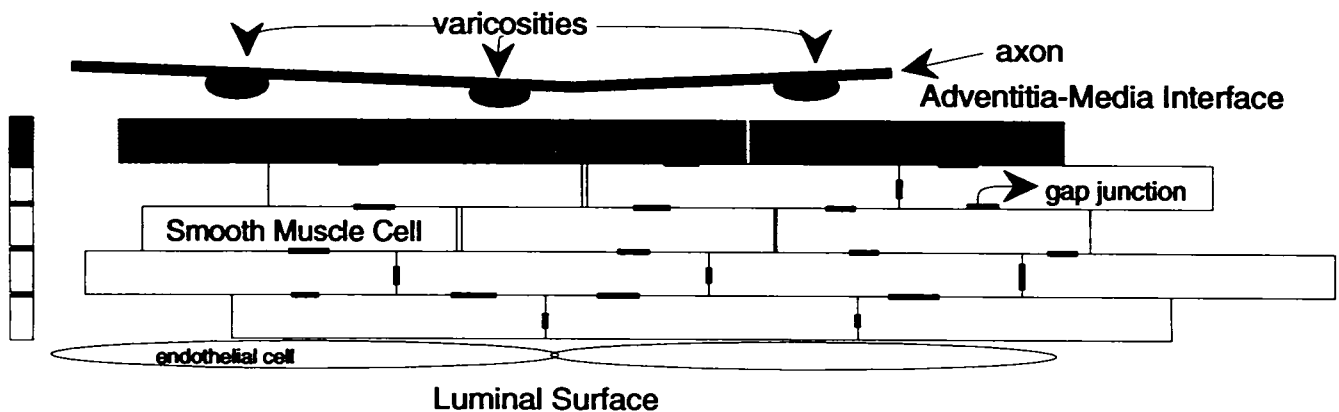

FIGURE 1 Illustration of the vascular wall of a small resistance vessel. A generalized morphology is shown that has axonal processes at the Adventitia-Media border of the vessel. Only the smooth muscle cells at the surface of the interface between the Adventitia and Media are near persynaptic terminals (varicosities). Four layers of smooth muscle cells are depicted with the cells interconnected via gap junctions. Only the outer most cells (Adentitia-Media border) are activated by neurotransmitter release from the varicosities. After receptor activation in these outer-most cells, these same cells rapidly (for our purposes instantaneously) produce a second messenger (*shaded* region). The second messenger then diffuses through the intracellular space and gap junction channels into neighboring cells. Because all the cells of the surface are simultaneously activated, diffusion out of this layer into the next can be treated as a one-dimensional diffusion case. The rectangular linear array at the left depicts the one dimensional case. Endothelial cells cover the smooth muscle cells at the luminal surface.

the channel. Modulation in the model will be represented only through its effects on the open probability p. The maximum permeability is then $P_{max} = Np$.

The gap junction channel is thought to consist of two hemichannels in series, one hemichannel being contributed by each of the two cells that make the whole channel. Further, each hemichannel has its own gate; we assume that the two gates are independent. The open probability p of the whole channel can then be written as $p = p^+p^-$, with p^+ being the open probabilities of the two hemichannels. In formulating the effects of modulation on the hemichannel probabilities, we will further assume that p^+ depends only on C^+ and similarly that p^- depends only on C^-. We are thus assuming that each hemichannel gate is affected only by the concentration of the modulator that it "sees" in its own cell. The actual mechanism of modulation can be accomplished either by occupancy of a binding site on the hemichannel by a putative second messenger or, alternatively, by phosphorylation of a binding site by a second messenger-activated protein kinase.

A further tacit assumption is that the occupancy of the hemichannel binding site by the second messenger molecule and the subsequent changes in junctional permeability take place instantaneously. If these events occur rapidly (milliseconds) relative to the timescale of the diffusion (many seconds), then this assumption should be a good one.

In the absence of modulators, the hemichannels have a nascent probability p_n of being open, and $q_n = 1 - p_n$ of being closed. The corresponding nascent permeability is $P_{max} = Np_n^2p$. We place no restriction on the exact kinetic scheme of closed and open states. However, we will assume that the up-modulator will affect the nascent kinetic scheme only by introducing new open configurations (i.e., new open states in the Markov scheme). The kinetic parameters in the original nascent scheme are thus assumed to be unaffected by the presence of the up-modulator. Given this, consider the closed probability q in the presence of up-modulator. Because all bound states are open, the hemichannel can close only if it is unbound. The closed probability q will then be given by $q = q_n[U]$, where $[U]$ is the probability that the channel is unbound or the fraction of unbound hemichannels.

Similarly, we can consider the effects of a down-modulator. Analogous to the case of the up-modulator, we will assume that the down-modulator will introduce only closed states into the nascent kinetic scheme. The open probability in the presence of down-modulator is then given by $p = p_n[U]$, because the hemichannel can open only if it is unbound.

We now need an expression for the fraction $[U]$ of hemichannels that are unbound. In the calculations presented here, we will assume that all of the hemichannel binding sites for the modulator are independent. Then, by standard enzyme kinetics, we find $[U] = k_{1/2}/(k_{1/2} + C)$, where $k_{1/2}$ is the concentration of modulator where one-half of the independent binding sites are occupied.

The permeability coefficient P is then given as below:

(1) no modulation:

$$P = P_{max}p_n^2,\qquad(4)$$

(2) up modulation:

$$P = P_{max}\left(1 - \frac{q_nk_{1/2}}{k_{1/2} + C^+}\right)\left(1 - \frac{q_nk_{1/2}}{k_{1/2} + C^-}\right)\qquad(5)$$

(3) down modulation:

$$P = P_{max}\left(\frac{p_nk_{1/2}}{k_{1/2} + C^+}\right)\left(\frac{p_nk_{1/2}}{k_{1/2} + C^-}\right).\qquad(6)$$

Equations 1, 2, and 4–6 define the system completely. The initial conditions are $C = C_{inj}$ inside the injected cell, and $C = 0$ for all the other cells at the initial time $t = 0$. The restriction of a zero concentration of modulator at $t = 0$ can be relaxed to allow a nascent uniform concentration of modulator in all cells (see Including the effects of a nascent modulator concentration, below).

Numerical solution

Ramanan and Brink (1990) presented an analytical solution to the above set of equations when the diffusing substance does not modulate the junction,

i.e., in the case shown in Eq. 4 above. However, when there is modulation (Eq. 5 or 6), we have not been able to solve the model analytically. Therefore, we have resorted to numerical methods.

Each cell is divided into $2R$ segments, and thus has $(2R + 1)$ gridpoints. We have chosen R to be 10 in all our computations. The leftmost and rightmost points in each cell are at the junctional membranes. The grid is numbered thus: the leftmost point (representing the adventitial-medial surface) of the injected cell is point 0; the points 0 to $2R$ are in the injected cell, and the ith cell to the right ($i > 0$) have the points in the inclusive range from $2iR + i$ to $2R(i + 1) + i$, for a total of $(2R + 1)$ points. The spatial resolution is then $\delta x = 2a/(2R)$. We iterate with time steps of $\delta t = 0.5(\delta x)^2/D$ (Crank, 1975, p. 145).

Let $C_n(j)$ denote the concentration of the diffusing substance at time $n\delta t$ at the point j. Equation 1 in Crank-Nicholson form (Crank, 1975, Sec. 8.5) is

$$(1 + 2\alpha)C_{n+1}(j) - \alpha\{C_{n+1}(j-1) + C_{n+1}(j+1)\}$$
$$= (1 - 2\alpha)C_n(j) + \alpha\{C_n(j-1) + C_n(j+1)\},\qquad(7)$$

where $\alpha = D\delta t/(\delta x)^2$, and the point j is not a junctional point, i.e., $j \neq 2iR + i$ for $i > 0$, $j \neq 2R(i + 1) + i$ for $i \geq 0$. Note that the system is symmetric about $x = 0$ (Eq. 3); this is achieved by replacing $C_{n+1}(-1)$ by $C_{n+1}(1)$ in the equation for $j = 0$.

Equation 2 can be discretized similarly. We follow the procedure given in Crank (1975, Sec 8.6). Consider a point labeled l corresponding to the left of a junction, i.e., $l = 2R(i + 1) + i$ for some $i \geq 0$. Let the label r stand for the point to the right of the junction, i.e., $r = l + 1$. Further, define ($l + 1$) to be the label of a "fictitious" point δx to the right of the junction. Although this point is to the right of the junction, we consider it to "belong" to the cell to the left of the junction, as in Crank (1975, Sec 8.6, discussion preceding Eq. 8.23). We can then write

$$\frac{C_n(l+1) - C_n(l-1)}{2\delta x} = \frac{P}{D}(C_n(r) - C_n(l)),$$

$$\frac{C_{n+1}(l+1) - C_{n+1}(l-1)}{2\delta x} = \frac{P}{D}(C_{n+1}(r) - C_{n+1}(l)),$$

these being the discretization of Eq. 2 for times $n\delta t$ and $(n + 1)\delta t$, respectively. Eliminating the fictitious values $C_n(l + 1)$ and $C_{n+1}(l + 1)$ can be done by use of Eq. 1. This, from the above paragraph, discretizes into

$$(1 + 2\alpha)C_{n+1}(l) - \alpha\{C_{n+1}(l-1) + C_{n+1}(l+1)\}$$
$$= (1 - 2\alpha)C_n(l) + \alpha\{C_n(l-1) + C_n(l+1)\}$$

Eliminating the fictitious values between the three equations above gives the permeability equation at the left boundary of the junction. A similar procedure can be carried out at the right junctional boundary. Thus, we finally get for the discretized Eq. 2:

$$-\alpha C_{n+1}(l-1) + (0.5 + \alpha + \beta)C_{n+1}(l) - \beta C_{n+1}(r)$$
$$= \alpha C_n(l-1) + (0.5 - \alpha - \beta)C_n(l) + \beta C_n(r)$$
$$-\beta C_{n+1}(l) + (0.5 + \alpha + \beta)C_{n+1}(r) - \alpha C_{n+1}(r+1)$$
$$= \beta C_n(l) + (0.5 - \alpha - \beta)C_n(r) + \alpha C_n(r+1)\qquad(8)$$

In the above, $\beta = \beta(l, r) = \alpha\delta xP(l, r)/D$, and the permeability $P = P(l, r)$ is computed from $C(l)$ and $C(r)$ by Eqs. 4–6 with the substitutions $C^+ = C_n(r)$ and $C^- = C_n(l)$.

Note that the discretized equations conserve concentration, as expected. The concentration at the end of the timestep can be found from the concentration at the beginning of the timestep by a matrix inversion algorithm. Because the equations have a tridiagonal form, we use the SGTSL routine from LINPACK for advancing one timestep. After each timestep, we check that the concentration is conserved to within 0.1%. Because all the matrices have to be finite, we find the solution only up to 10 cell lengths from the injected cell. This has proven to be sufficient to conserve the concentration until the maximum time that we have followed the diffusion.

All routines were written in Objective-C. The LINPACK routines were converted to C using the *f2c* program. Computation times were 1 s for following the diffusion up to 40 s, with the parameters in the results section. All computations and displays were done in NeXTStep. Three-dimensional plots (Fig. 2) were done with the use of Wolfram's *Mathematica* (Wolfram Research Inc., 1991).

Effective diffusion coefficient

Consider the case where diffusing substance uniformly fills the region $-2a \leq x \leq 2a$ at a concentration C_{imp}, and there are no junctional membranes. This problem has been solved in Crank (1975, p. 15). The resulting equation for the concentration is

$$C(x, t) = \frac{C_{imp}}{2} \left\{ \text{erf} \frac{2a - x}{2\sqrt{Dt}} + \text{erf} \frac{2a + x}{2\sqrt{Dt}} \right\}. \tag{9}$$

A measure of the spread of substance at time *t* is given by

$$S = \int_{-x}^{x} dx \, x^2 \frac{C(x, t)}{4aC_{imp}}. \tag{10}$$

This can be evaluated explicitly, yielding $S = (2Dt + 4a^2/3)$. Inverting this equation for D yields

$$D = \frac{1}{6t} \{3S - 4 a^2\}. \tag{11}$$

Equation 11 can be used to define an effective diffusion coefficient D_{eff} for our model. The system of Eq. 9 is symmetric about $x = 0$; hence, the profile for $x > 0$ would be the counterpart of our model without junctions, if we interpret $2a$ (rather than $4a$) in Eq. 9 to stand for the width of the cells. As opposed to the model of Eq. 9, D_{eff} will not be constant over time for our model, incorporating as it does a junctional permeability that, moreover, varies dynamically with time. However, it provides a useful measure to summarize the results as various parameters are varied. In all the cases we have studied, D_{eff} varies less than 3% in the range of times from 10 to 40 s.

Including the effects of a nascent modulator concentration

In our modeling, we present results only for cases where the injected cell has a uniform concentration of modulator and all other cells have no modulator present at time $t = 0$. Consider, however, the case where there is a nascent concentration of up-modulator C_a at time $t = 0$ in all cells. Eqs. 1 and 2 are not affected by an additive change in C. However, the permeability P is sensitive to the absolute value of the modulator concentration (see Eqs. 5 and 6). If, however, we can find parameters q' and k' such that the equation

$$q' \frac{k'}{C + k'} = q \frac{k}{C + C_a + k} \tag{12}$$

holds for all C, then the problem can be transformed into the formalism for zero nascent concentration. This is indeed possible; solving for the primed quantities yields $k' = C_a + k$ and $q' = (qk)/k'$, which are independent of C. Similarly, for a down-modulator, we solve for the primed quantities in the equation

$$p' \frac{k'}{C + k'} = p \frac{k}{C + C_a + k}, \tag{13}$$

giving $k' = C_a + k$ and $p' = (pk)/k'$.

Thus, using these transformations, the results in the presence of a nascent concentration of modulator can be found from those for zero nascent modulator.

The diffusion of nitric oxide

We will assume that a spherical region of radius 5 μm is filled with a uniform concentration C_{imp} of nitric oxide caused, e.g., by pulsatile release from a nonadrenergic noncholinergic neuronal varicosity. Because the gas is very soluble in lipid (3 times more so than in water), there are no barriers to its diffusion in any direction; we have chosen, therefore, to model its diffusion as an unimpeded one in three dimensions. The gas is assumed to decay with a half-life τ of 5 s. This problem has been solved (Crank, 1975, p. 29); the solution is

$$Ce^{1.7} = \frac{1}{2} C_{imp} \left\{ \text{erf} \frac{a + r}{2\sqrt{Dt}} + \text{erf} \frac{a - r}{2\sqrt{Dt}} \right\} \\ - \frac{C_{imp}}{r} \sqrt{\left(\frac{Dt}{\pi}\right)} \left[\exp\left\{ -\frac{(a - r)^2}{4Dt} \right\} - \exp\left\{ -\frac{(a + r)^2}{4Dt} \right\} \right]. \tag{14}$$

RESULTS

Our preliminary modeling studies have demonstrated several important phenomena. The most critical elements in the model concern the interrelationships between $C_{imp}/k_{1/2}$ and p_a and their respective effects on the intercellular diffusion of putative second messenger molecules/ionic species, as reflected by the value of D_{eff}. The nature of these interrelationships is illustrated in the three-dimensional graphs shown in Fig. 2 *D*. The *x* axis represents the open probability (p_a) of the gap junction channels, and the log of $C_{imp}/k_{1/2}$ is plotted along the *y* axis. D_{eff} (cm^2/s) is plotted on the *z* axis.

The topography of up regulation (darkest shading) functions over a more limited range than the surface representing down regulation (the least shadowed surface). The maximum value of D_{eff} is limited by the mobility of the messenger within the cytosol of the cells and the maximum junctional permeability P_{max}. Down regulation is limited under normal conditions not by the mobility of the diffusing molecule in the cytosol but by the increased closed probability of the gap junction channels (q_a). In all of the modeling shown, D was set to 10^{-7} cm^2/s and P_{max} was set to 8×10^{-5} cm/s. These values are similar to those assumed by Tsien and Weingart (1976) (see also Brink, 1991). The width of the cell ($2a$) was set to 10 microns.

On the definition of D_{eff}

D_{eff} is a composite term reflecting the net effects of both the cytoplasmic diffusion coefficient and the junctional permeability. Canonically, an effective diffusion coefficient D_{eff}^{canon} has been defined as $1/D_{eff}^{canon} = 1/D + 1/(2aP)$ (Weidmann, 1966). This definition is based on analogy to electrical resistances, the "series resistances" of the cytoplasm ($1/D$) and the junction ($1/(2aP)$) adding to yield the total effective resistance ($1/D_{eff}^{canon}$). We have defined D_{eff} explicitly in the Materials and Methods based on a measure of the spread of the substance, using the spread in a junctionless membrane as a baseline for comparison. Although the canonical definition cannot be used in the cases where the junctional permeabilities vary dynamically, we can compare the canonical definition with our definition in the case of drugs that do not modulate the junction. For such drugs, we have $(1/D_{eff}^{canon}) = 1/D + 1/(2ap_a P_{max})$.
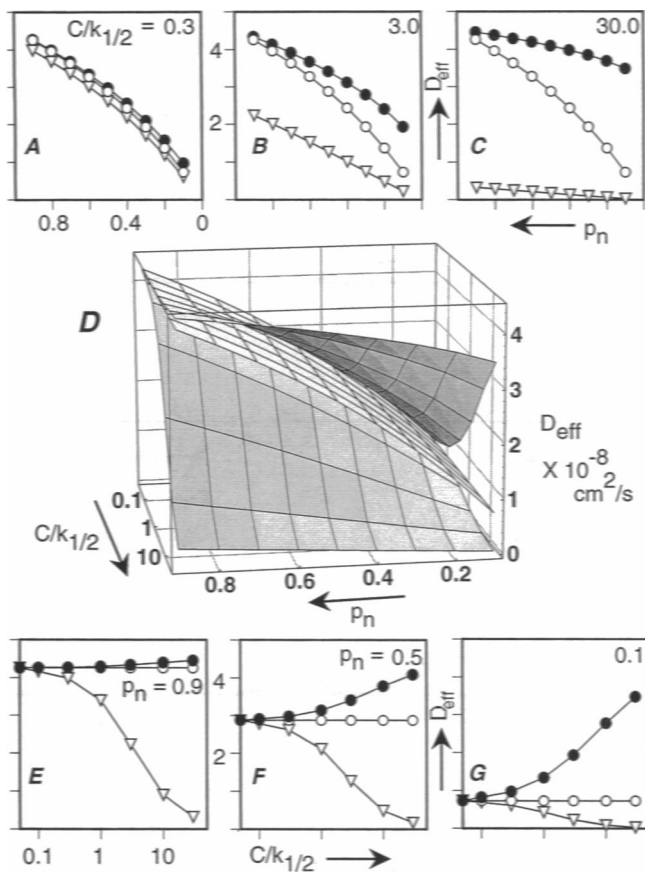
FIGURE 2   (A–C) The effects of up- and down regulation can be observed over a wide range of physiologically relevant conditions. All panels compare the calculated D_{eff} values (cm²/s) for up regulation (●), no regulation (○), and down regulation (∇), for a broad spectrum of p_n values, at three $C_{\text{imp}}/k_{1/2}$ values; 0.3 (panel A), 3.0 (panel B), and 30 (panel B). For these graphs, values of D_{eff} were calculated 40 s after stimulation, with $D = 10^{-7}$ cm²/s, and $P_{\text{max}} = 8 \times 10^{-5}$ cm/s. (D) Three-dimensional graph of the results of the model. The x axis represents the nascent probability p_n that a channel is open. The y axis is the unitless parameter $C_{\text{imp}}/k_{1/2}$ in a log scale, where C_{imp} is the concentration of the diffusing substance at the initial time and $k_{1/2}$ is the concentration of substance at which half of the hemichannels are occupied by the substance. The z axis is the effective diffusion coefficient D_{eff} in units of 10^{-8} cm²/s; D_{eff} is a composite measure of the effects of both diffusion and membrane permeability. The upward curving sheet is for substances that up-modulate gap junction channels in the junctional plaque (cause an increase in the open probability of the channels); the bottom sheet is for down-modulators, and the sandwiched sheet is for substances that do not modulate gap junction channels. The graph shows that down-modulators have influence over a broader range of conditions than do the up-modulators. (E–G) Down regulation is more prominent under more diverse physiological conditions. All panels compare the calculated D_{eff} values (cm²/s) for up regulation (●), no regulation (○), and down regulation (∇) for a broad range of $C_{\text{imp}}/k_{1/2}$ values, at three distinct values of p_n; 0.1 (panel G), 0.5 (panel F; thought to be the most likely condition in cells; see Results), and 0.9 (panel E). For these graphs, values of D_{eff} were calculated 40 s after stimulation, with $D = 10^{-7}$ cm²/s, and $P_{\text{max}} = 8 \times 10^{-5}$ cm/s.

We have fitted the results for nonmodulating drugs to a linear regression of $1/D_{\text{eff}}$ (as given by Eq. 11) against $1/p_n$ with the form $1/D_{\text{eff}} = A + B/p_n$. If the canonical definition agrees with the one in Eq. 17, then we expect that $1/A = D$ and $1/B = 2aP_{\text{max}}$. The fit we get is indeed linear with $r =$

0.999999. Further, the fit gives $1/A = 1.08 \times 10^{-7}$ cm²/s and $1/B = 7.82 \times 10^{-7}$ cm²/s. This agrees with the expected values, $D = 10^{-7}$ cm²/s and $2aP_{\text{max}} = 8 \times 10^{-7}$ cm²/s.

Although we are concentrating in this paper on the influence of dynamically varying permeabilities on the spread of substance and, thus, on D_{eff}, we note that even when $p_n = 0.5$, the cytosolic diffusion coefficient makes up about 1/3 of the total effective diffusion coefficient. This contribution would increase to about 1/2 for high $C/k_{1/2}$ for a range of p_n for the up-modulator (see Fig. 2 D). The actual contribution would vary, of course, from those given here depending on the actual values of the diffusion coefficient D and the maximum permeability P_{max} for the experimental system.

$C_{\text{imp}}/k_{1/2}$ determines the magnitude of the effect of the up- and down-regulators for any given value of p_n

As shown in Fig. 2 A–C, when the $C_{\text{imp}}/k_{1/2}$ ratio is low (e.g., 0.3; Fig. 2 A), there are no measurable effects of either up- or down-modulators on the effective diffusion coefficient (D_{eff}), for any given p_n. This is an important observation, because it indicates that under low resting levels of the putative intracellular modulator, or similarly, after low levels of cellular activation, the primary determinant of intercellular communication, or D_{eff}, is p_n. However, as the $C_{\text{imp}}/k_{1/2}$ ratio increases, so do the effects of both up- and down-modulators on D_{eff}. For example, at a $C_{\text{imp}}/k_{1/2}$ of 3.0 (Fig. 2 B), the effects of up regulation are only noticeable at the lower open probabilities ($p_n = 0.1$–0.2), whereas in contrast, the effects of down regulation are visible throughout the entire spectrum of p_n. At high $C_{\text{imp}}/k_{1/2}$ ratios (e.g., 30; Fig. 2 C), the effects of up regulation are noticeable at $p_n = 0.5$, but down-regulators again appear to exert more important effects on D_{eff} throughout the spectrum of open probabilities. However, it is clear that both up- and down-regulators are capable of eliciting two- to fourfold changes in D_{eff} under physiologically relevant conditions (see Discussion).

p_n governs the physiological importance of up- or down-regulators

As shown in Fig. 2 E–G, at the lowest values of p_n (0.1, Fig. 2 E) the effects of up-regulators are more pronounced than those of down-regulators. However, as p_n is increased, the effects of up- and down-regulators become more symmetrical (0.5, Fig. 2 F) until, eventually, the effects of up regulation are trivial, and down regulation predominates (0.9, Fig. 2 G).

Cell state dependence of the effects of up- and down-regulators on intercellular diffusion and recruitment of coupled cells: intercellular diffusion profiles after cellular activation

The descriptions above demonstrate the potential complexities of the regulation of intercellular communication among

coupled cells. However, a more detailed analysis of two ex-
amples, in particular, will suffice to demonstrate the impor-
tance of the cell state dependence of the effects of junctional
modulators on the degree of intercellular communication.

Case 1. The anticipated effects of up-, down-, or no regu-
lation on intercellular diffusion of second messenger
molecules/ions, under physiologically relevant conditions
(p_a = 0.5, Veenstra and DeHaan, 1986; Manivannan et al.,
1992), are displayed in Fig. 3. We have set $C_{imp}/k_{1/2}$ = 3.0;
the profiles do not significantly differ over the expected nor-
mal range of 0.5–3 for $C_{imp}/k_{1/2}$. Note that as expected, for the
same increase in intracellular second messenger levels, up
regulation of junctional communication was associated with
a greater fraction of the initial second messenger concen-
tration in cells further removed from the source of activation
than that observed for either the down regulation or no regu-
lation cases.

Case 2. The effects of up- and down regulation are very
different if the p_a is altered. For example, Fig. 4 depicts the
expected diffusion profiles when $C_{imp}/k_{1/2}$ is once again 3.0,
but p_a = 0.1 in the case of the up-regulator, whereas p_a =
0.9 in the case of the down-regulator. Under these conditions,
the intercellular diffusion profile in the presence of a down-
regulator is clearly more spread out than that observed for the
up-regulator, or no regulation. This is despite the fact that the
messenger depletion in the injected cell is clearly less with
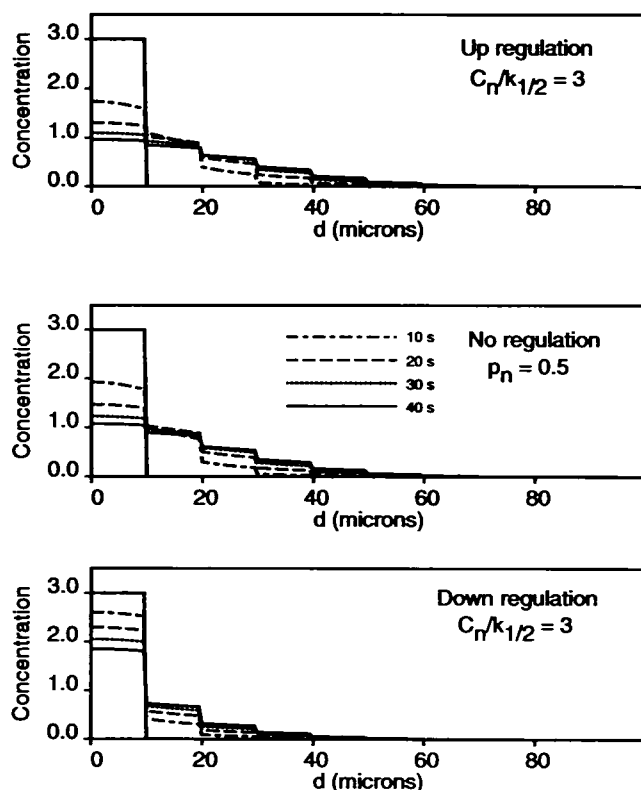

FIGURE 3   Comparison of intercellular diffusion profiles for up regula-
tion, down regulation, and no regulation, under the presumably most physi-
ologically relevant conditions. $C_{imp}/k_{1/2}$ = 3, and p_a = 0.5 in all cases. The
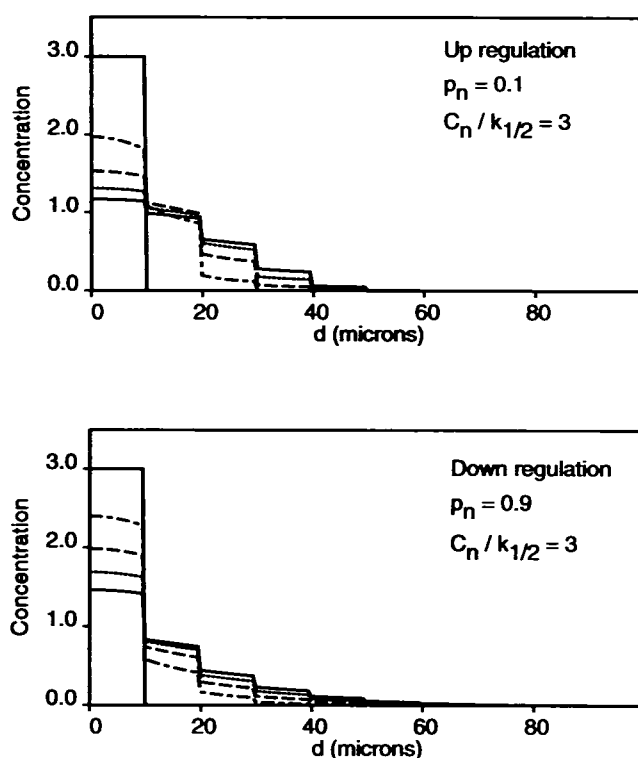initial concentration C_{imp} is 3 units.

FIGURE 4   The physiological effects of up- and down-regulators are cell
state-dependent. Comparison of intercellular diffusion profiles for an up-
regulator and down-regulator under physiologically diverse conditions. This
graph demonstrates that under certain conditions, a down-regulator will
actually be associated with greater intercellular diffusion of an intracellular
second messenger. $C_{imp}/k_{1/2}$ = 3 for both the up-regulator and the down-
regulator. p_a = 0.1 for the up-regulator, whereas p_a = 0.9 for the down-
regulator. The initial concentration C_{imp} is 3 units.

down regulation. The reason for this is that, for down regu-
lation, the high concentration of messenger causes the junc-
tion in the injected cell to have a low permeability. However,
any messenger diffusing into the adjacent cells spreads away
faster because the low initial concentration in the adjacent
cells makes their junctional permeability high. For the up-
regulator, however, the rapid depletion from the initial cell
because of its high junctional permeability is not enough to
make up for the low permeability of the junctions between
cells that are initially unfilled. The net result is that D_{eff} for
the down-regulator, under these conditions, is actually more
than 2 times greater than that for the up-regulator. That is,
for the same increase in intracellular second messenger lev-
els, down regulation was actually associated with a greater
fraction of the initial second messenger concentration in cells
further removed from the source of activation, than that ob-
served for either the up regulation or no regulation cases.

Accounting for the effects of rapidly inactivated messenger molecules

For all of the aforementioned examples, we have assumed that
the second messenger molecule/ionic species of interest
is stable and, thus, that there is no significant loss of the

messenger molecule over the time course of the diffusion response. For many intercellular messenger molecules, this is indeed thought to be the case. However, it is also conceivable that important intracellular messenger molecules can be rapidly inactivated and/or metabolized. For such unstable molecules, the intracellular concentration and intercellular diffusion profile would be more dramatically altered as a function of both time and distance away from the activated cell. One relevant example of such a molecule would be nitric oxide, a ubiquitously distributed neurotransmitter molecule, which has demonstrable physiological roles in a host of biological processes. Therefore, we modified the model (see Eq. 14 in Materials and Methods) to account for the intercellular diffusion of nitric oxide a putative neurotransmitter, with a half-life of 5 s and a diffusion coefficient of 5×10^{-5} cm^2/s. Fig. 5 shows the diffusion profile in the style of Crank (p. 30, Fig 3.1). The figures plot the normalized concentration C/C_{imp} against normalized distance x/a from the center of the cell. The various curves are labeled by the dimensionless time $(Dt/a^2)^{1/2}$. The parameter θ that distinguishes the various figures is a dimensionless inverse time constant $a^2/\tau D$. For the specific case considered here, $\theta = 4 \times 10^{-3}$. The profiles for this values of θ are indistinguishable from the ones for $\theta = 0$ for the times shown. Note that the labels $(Dt/a^2)^{1/2}$ with a value of 1 correspond here to a time

of 0.02 s. Fig. 5 (*top*) illustrates that diffusion of nitric oxide occurs very rapidly, such that only 8% of the original nitric oxide concentration remains 20 ms after stimulation (0.5% after 50 ms). This reflects the fact that nitric oxide is a highly lipophilic molecule with unimpeded three-dimensional diffusion characteristics (see Materials and Methods). Because the time course for the diminution in the original nitric oxide concentration caused by the spread of nitric oxide in three dimensions is three orders of magnitude greater than the half-life for its metabolic decay (i.e., 5 ms vs. 5 s; see Fig. 5), one main implication of our modeling is that the lipophilicity of nitric oxide is a more important determinant of its limited diffusion profile than its rapid metabolic loss. In fact, our model predicts that nitric oxide will not effectively diffuse further than its nearest neighbor cell; this is reflected by the fact that the second cell removed will see at most only 1% of the original nitric oxide concentration (see Fig. 5). Note that the diffusion characteristics of nitric oxide are drastically different from the diffusion of less lipophilic second messenger molecules in anisotropic cells (see Figs. 3 and 4).

DISCUSSION

The model has several important applications to the understanding of tissue physiology, and these are discussed below.
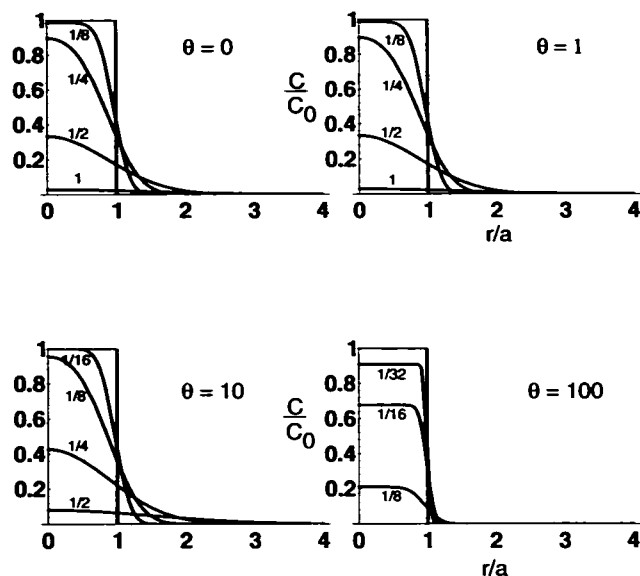

FIGURE 5 Modified model for predicting the intercellular diffusion of the chemically unstable messenger molecule nitric oxide. Because the gas is readily soluble in lipid and water, we have modeled it as diffusing freely in three dimensions. At the initial time, the gas is assumed to fill uniformly a sphere with a concentration C_{imp}. The graphs plot the normalized concentration C/C_{imp} against the normalized distance r/a from the center of the injected cell; a is the radius of the injected cell. The labels against the various curves are the values of $(Dt/a^2)^{1/2}$. The parameter θ is a dimensionless inverse half-life given by $a^2/\tau D$, where τ is the half-life of the diffusing substance. For nitric oxide, typical values for the parameters are: $D = 5 \times 10^{-5}$ cm^2/s and $\tau = 5$ s. For these values, $\theta = 0.004$ and $(Dt/a^2)^{1/2} = 1$ corresponds to 20 ms. The profiles show that the rapid diffusion of the gas reduces its concentration to about 8% of its initial concentration in about 20 ms (and less than 1% in 50 ms, not shown).

The observed changes in D_{eff} are likely to be physiologically important

Undoubtedly, the extent of intercellular communication among cells in tissues would be expected to play a major role in the coordination of tissue responses (see Introduction; Hall et al., 1993). The question we are really asking is the following: What kind of change in D_{eff} might be physiologically relevant? Of course, the answer will vary depending on the particular tissue of interest, but practically speaking, we suggest that at least a two- to fourfold change in D_{eff} would probably be required. Roughly, a fourfold change in D_{eff} would be associated with a doubling of the number of cells recruited into the functional syncytial unit in any one plane of diffusion. In light of the range of changes in D_{eff} predicted by the model (fivefold for both up- and down-regulators; see Fig. 2), it seems reasonable to assume that such changes in D_{eff} might have a significant impact on the coordination of cellular responses (e.g., secretion, contraction, relaxation, etc.) in poorly innervated tissues that lack the capacity for regenerative electrical events (i.e., propagated action potentials). Such a mechanism would be of obvious importance to the coordinated function of any tissue that is wholly or partially dependent on intercellular communication through gap junctions.

The model conditions required to elicit physiologically relevant changes in intercellular diffusion profiles are commonly observed in cells

It can be argued that two- to fourfold changes in D_{eff} are sufficient to produce significant and physiologically relevant

changes in the extent of intercellular communication and, thus, the number of recruited cells. However, the next question is: Do the conditions required to produce such changes in D_{eff} actually exist inside living cells? The answer to this question is yes. For example, the 3- to 10-fold changes in the intracellular concentrations of second messenger molecules/ ions that produce the necessary effects on D_{eff} in the model (see Figs. 3 and 4) are commonly reported in the literature after cellular activation by diverse stimuli (e.g., changes in intracellular calcium and/or cAMP and/or cGMP). Additionally, all of the estimates for cytoplasmic diffusion and junctional permeability utilized in the model to calculate the intercellular diffusion profiles are based on existing experimental data. Moreover, as illustrated in Fig. 2, two- to fourfold changes in D_{eff} can occur over a wide range of physiological conditions. It is important to point out that the model can actually partially explain some of the observed variability in the effects of second messengers on junctional permeability. For example, because D_{eff} is very dependent on p_n, there will be significant changes in the diffusion profiles if p_n varies significantly among distinct tissues with similar gap junction proteins (i.e., two- to threefold change in p_n). That is, the cell state dependence of the effects of up- and down-regulators (see Figs. 2–4) can explain, at least in part, why the same second messenger molecule has been observed to have differing effects on junctional permeability in different cells (De Mello, 1988; Moore et al., 1991; Takens-kwak and Jongsma, 1992; Moreno et al., 1992, 1993).

Down regulation of intercellular communication is likely to be more physiologically important than up regulation

Another clear conclusion from our data is that down regulation produces changes in D_{eff} that are more likely to be physiologically relevant (i.e., twofold changes in D_{eff}) over a wider range of conditions (with respect to both the $C_{\text{imp}}/k_{1/2}$ and p_n) than the changes in D_{eff} observed for up regulation (see Figs. 2–4). This is not unexpected, because the model is based on physiological and physical realities that seem to favor down regulation. For example, the maximum value of D_{eff} (9.3 × 10^{-8} cm²/s) is limited by the maximum value of the macroscopic junctional permeability. The value of P_{max} used in these studies (8 × 10^{-5} cm/s) was partly based on our previous work (Brink and Ramanan, 1985; Ramanan and Brink, 1990) and was determined by the following: 1) measurements of intercellular diffusion of ions and fluorescent dye molecules through the aqueous environment of the gap junctional channel, and 2) estimates of the size of gap junctional plaques observed in different tissues (Christ et al., 1993). Thus, although the maximum value of D_{eff} is likely only to be increased severalfold over the presumed resting values, in contrast, the minimum value of D_{eff} can be decreased by many orders of magnitude; as $C_{\text{imp}}/k_{1/2}$ of a down-regulator approaches infinity and p_n approaches zero.

Implications for vascular physiology

It is well documented that relaxation is faster than contraction. One possible explanation for this observation (in smooth muscles that are tonically contracted, have low innervation densities, and have no capacity for regenerative electrical events; i.e., total dependence on gap junctions for syncytial tissue responses) is that during the tonically contracted state most of the junctional channels are open. That is, contracting stimuli are up-regulators, and during a steady-state contraction the cells are well coupled ($p_n = 0.5$). Thus, initiation of a relaxing stimulus (even if the stimulus is a down-regulator) will result in a rapid intercellular transit of the relaxing stimulus, favoring a quick relaxation response (see Fig. 3). Therefore, contractile response generation can be seen as a relatively slow recruitment of cells into the functional syncytial unit, coinciding with an increase in junctional permeability. Conversely, relaxation can be seen as a rapid intercellular spread of a second messenger through gap junctions.

Implications for nitric oxide biology

The literature abounds with recent reports concerning the importance of nitric oxide to tissue biology (Palmer et al., 1988; Ignarro, 1989; Lancaster, 1992; Said, 1992; Rajfer et al., 1992; Burnett et al., 1992; Azadzoi et al., 1992). Specifically, nitric oxide has been described as a neurotransmitter released from nonadrenergic, noncholinergic neurons (NANC) in a host of peripheral tissues, where it is thought to be an important smooth muscle relaxant (Lancaster, 1992; Said, 1992; Rajfer et al., 1992; Burnett et al., 1992; Azadzoi et al., 1992). Onset of smooth muscle relaxation is thought to be elicited by nitric oxide diffusion into smooth muscle cells, the activation of soluble guanylate cyclase, subsequent increases in intracellular cGMP levels, and corresponding decreases in smooth muscle tone. In this regard, our results demonstrate a very small effective diffusion radius for nitric oxide (Fig. 5) and indicate that if the observed relaxing activity of nitric oxide were caused by a direct action of nitric oxide on all of the smooth muscle cells, then a very intimate neuronal innervation pattern would be required (i.e., 1:1 ratio of neuron to smooth muscle cell). Such intimate neuronal innervation would be required because our modeling studies indicate that nitric oxide spreads too quickly to be of physiological significance to any cell other than the nearest neighbor of the neuronal source. Because such an intimate neuronal innervation pattern is not likely to be characteristic of all peripheral tissues, how might nitric oxide exert its known biological effects on cells distantly removed from the source of activation? We propose that syncytial relaxation in poorly innervated peripheral tissues is achieved as follows: nitric oxide diffuses only into cell(s) nearest the vicinity of the innervating nerve process, and it is the intercellular diffusion of cGMP (cyclic guanosine monophosphate) to distant cells that is the relevant messenger species responsible for mediating syncytial smooth muscle relaxation responses. This

seems a plausible explanation given the stability of cGMP relative to nitric oxide, and the fact that cGMP is freely permeable through gap junctions.

Future areas of research

In addition to the examples described above, there are also potential applications of the model to other important tissue functions known to be wholly or partially dependent on intercellular communication through gap junctions: embryonic development, coordination of pancreatic secretions, myometrial contractions, and possibly tumor formation and/or progression (see Introduction). Moreover, because many cell types are anisotropic, this model should have broad applications to a host of tissues. However, until we have more empiric observations on which to base our model, further discussion seems unwarranted.

Moreover, it should be pointed out that the current model does not account for some likely complications of the intracellular environment. For example, what happens when more than one second messenger simultaneously affects junctional permeability? Or what occurs when there is cooperativity among hemichannel binding sites? Additionally, the model does not take into account the possibility that intercellular diffusion of second messenger molecules can elicit regenerative second messenger waves, similar to the propagated calcium waves seen between coupled cells (Christ et al., 1992). Thus, the model might in fact significantly underestimate the concentration of second messenger molecules in distantly removed cells. However, despite these potential limitations, the model represents an important conceptual advance in our understanding of how dynamic changes in the extent of intercellular communication might have a significant biological impact on coordinated tissue function, under a variety of physiologically relevant conditions. Moreover, the model provides us with a host of hypotheses that can be experimentally tested.

REFERENCES

Azadzoi, K. M., N. Kim, M. L. Brown, I. Goldstein, R. A. Cohen, and I. Saenz de Tejada. 1992. Endothelium-derived nitric oxide and cyclooxygenase products modulate corpus cavernosum smooth muscle tone. *J. Urology.* 147:220–225.

Barr, L., M. M. Dewey, and W. Berger. 1965. Propagation of action potentials and the structure of the nexus in cardiac muscle. *J. Gen. Physiol.* 48:797a. (Abstr.)

Brink, P. R. 1991. Gap junction channels and cell-to-cell messengers in myocardium. *J. Cardiovasc. Electrophys.* 2:360–366.

Brink, P. R., and S. V. Ramanan. 1985. A model for the diffusion of fluorescent probes in the septate giant axon of earthworm. *Biophys. J.* 48:299–309.

Burnett, A. L., C. J. Lowenstein, D. S., Bredt, T. S. K. Chang, and S. H. Snyder. 1992. Nitric oxide: a physiologic mediator of penile erection. *Science.* 257:401–403, 1992.

Chanson, M., and P. Meda. 1993. Rat pancreatic acinar cell coupling: comparison of extent and modulation in vitro and in vivo. *In* Gap Junctions, Progress in Cell Research. Vol. 3. Amsterdam. 199–205.

Christ, G. J., A. P. Moreno, C. M. Gondr, C. Roy, A. C. Campos de Carvalho, A. Melman, and D. C. Spray. 1993a. Gap junctions in human corpus cavernosum vascular smooth muscle: a test of functional significance. *In* Gap Junctions, Progress in Cell Research. Vol. 3. Edited by J. E. Hall et al. Amsterdam. 211–217.

Christ, G. J., P. R. Brink, W. Xhao, J. Moss, C. M. Gondr, C. Roy, and D. C. Spray. 1993b. Gap junctions modulate tissue contractility and alpha-1-adrenergic agonist efficacy in isolated rat aorta. *J. Pharmacol. Exp. Ther.* 266:1054–1065.

Christ, G. J., A. P. Moreno, A. Melman, and D. C. Spray. 1992. Gap junction-mediated intercellular diffusion of Ca^{2+} in cultured human corporal smooth muscle cells. *Am. J. Physiol.* 263:C373–C383.

Cole, W. C., R. E. Garfield, and S. J. Kirkaldy. 1985. Gap junctions and direct intercellular communication between rat uterine smooth muscle cells. *Am. J. Physiol.* 249:C20–C31.

Cornell-Bell, A. H., S. M. Finkbeiner, M. S. Cooper, and S. J. Smith. 1990. Glutamate induces calcium waves in cultured astrocytes: long range glial signalling. *Science.* 247:470–473.

Crank, J. 1975. The Mathematics of Diffusion. 2nd Ed. Clarendon Press, Oxford. 413 pp.

Daniel, E. E. 1987. Gap junctions in smooth muscle. *In* Cell-to-Cell Communication. Edited by W. C. De Mello. Plenum Press, New York. 149–185.

De Mello, W. C. 1988. Increase in junctional conductance caused by isoproterenol in heart cell pairs is suppressed by cAMP-dependent protein-kinase inhibitor. *Biochem. Biophys. Res. Commun.* 154:509–514.

Eghbali, B., J. A. Kessler, L. M. Reid, C. Roy, and D. C. Spray. 1991. Involvement of gap junctions in tumorigenesis: transfection of tumor cells with connexin 32 cDNA retards growth in vivo. *Proc. Natl. Acad. Sci. USA.* 88:10701–10705.

Hall, J. E., G. A. Zampighi, and R. M. Davis, editors. 1993. Gap Junctions, Progress in Cell Research. Vol. 3. Amsterdam.

Hirst, G. D. S., and F. R. Edwards. 1989. Sympathetic neuroeffector transmission in arteries and arterioles. *Phys. Rev.* 69:546–604.

Gibbins, I. L., J. L. Morris, J. B. Furness, and M. Costa. 1988. Innervation of systemic blood vessels. *In* Nonadrenergic Innervation of Blood Vessels. G. Burnstock and S. G. Griffiths, editors. CRC Press, Boca Raton, FL.

Ignarro, L. J. 1989. Biological actions and properties of endothelium-derived nitric oxide formed and released from artery and vein. *Circ. Res.* 65:1–21.

Kanno, Y. Modulation of cell communication, and carcinogenesis. 1985. *Jpn. J. Physiol.* 35:693–707.

Kanno, Y., Y. Sasaki, and Y. Shiba. 1993. Delayed change in gap-junctional cell communication in the acinus of the rat submandibular gland after secretion of saliva. *In* Gap Junctions, Progress in Cell Research. Vol. 3. Amsterdam. 207–210.

Lancaster, J. R., Jr. 1992. Nitric oxide in cells. *American Scientist.* 80: 248–259.

Larson, D. M., C. C. Haudenschild, and E. C. Beyer. 1990. Gap Junction Messenger RNA Expression by Vascular Wall Cells. *Circ. Res.* 66: 1074–1080.

Manivannan, K., S. V. Ramanan, R. T. Mathias, and P. R. Brink. 1992. Multichannel recordings from membranes which contain gap junctions. *Biophys. J.* 61:217–227.

Minkoff, R., V. R. Rundus, S. B. Parker, E. C. Beyer, and E. L. Hertzberg. 1993. Connexin expression in the developing avian cardiavascular system. *Circ. Res.* 73:71–78.

Moore, L. K., E. C. Beyer, and J. M. Burt. 1991. Characterization of gap junction channels in A7r5 vascular smooth muscle cells. *Am. J. Physiol.* 260:C975–C981.

Moreno, A. P., A. C. Campos de Carvalho, G. J. Christ, and D. C. Spray. 1993a. Gap junctional communication between human corpus cavernosum smooth muscle cells in culture: Gating behavior and single channel events. *Am. J. Physiol.* 264:C80–C92.

Moreno, A. P., G. I. Fishman, E. C. Beyer, and D. C. Spray. 1993b. Human Cx43 and human Cx45 expressed in a mammalian cell line: heterotypic

channels conserve the electrophysiological properties of hemichannels. Int. Meeting on Gap Junctions, p. 68., Hiroshima, Japan, August 24–27.

Moreno, A. P., G. I. Fishman, and D. C. Spray. 1992. Phosphorylation shifts unitary conductance and modifies voltage-dependent kinetics of human connexin43 gap junction channels. Biophys. J. 62:51–53.

Palmer, R. M. J., D. S. Ashton, and S. Moncada. 1988. Vascular endothelial cells synthesize nitric oxide from L-arginine. Nature. 333:664–666.

Rajfer, J., W. J. Aronson, P. A. Bush, F. J. Dorey, and L. J. Ignarro. 1992. Nitric oxide as a mediator of relaxation of the corpus cavernosum in response to nonadrenergic, noncholinergic neurotransmission. N. Engl. J. Med. 326:90–94.

Ramanan, S. V., and P. R. Brink. 1990. Exact solution of a model of diffusion in an infinite chain or monolayer of cells coupled by gap junctions. Biophys. J. 58:631–640.

Risek, B., S. Guthrie, N. Kumar, and N. B. Gilula. 1990. Modulation of gap-junction transcript and protein expression during pregnancy in the rat. J. Cell Biol. 110:269–282.

Saez, J. C., J. A. Connor, D. C. Spray, and M. V. L. Bennett. 1989. Hepatocyte gap junctions are permeable to the second messenger, inositol 1,4,5-trisphosphate, and to calcium ions. Proc. Natl. Acad. Sci. USA. 86:2708–2712.

Said, S. I. 1992. Nitric Oxide and vasoactive intestinal polypeptide: cotransmitters of smooth muscle relaxation. NIPS. 7:181–183.

Sanderson, M. J., A. C. Charles, and E. R. Dirksen. 1990. Mechanical stimulation and intracellular communication increases intracellular communication increases intracellular Ca^{2+} in epithelial cells. Cell Regulation. 1:585–596.

Segal, S. S., and B. R. Duling. 1986. Flow Control Among Microvessels Coordinated by Intercellular Conduction. Science. 234:868–870.

Sheridan, J. D. 1987. Cell communication and growth. In Cell-to-Cell Communication. W. C. De Mello, editor. Plenum Press, New York. 187–222.

Spear, J. F., C. W. Balke, M. D. Lesh, A. H. Kadish, J. H. Levine, and E. N. Moore. 1990a. Effect of cellular uncoupling by heptanol on conduction in infarcted myocardium. Circ. Res. 66:202–217.

Spear, J. F., C. W. Balke, M. D. Lesh, A. H. Kadish, J. H. Levine, and E. N. Moore. 1990b. Letters to the Editor. Circ. Res. 67:1299–1300.

Spray, D. C., and J. M. Burt. 1990. Structure-activity relations of the cardiac gap junction channel. Am. J. Physiol. 27:C195–C205.

Spray D. C., A. P. Moreno, M. Rook, G. J. Christ, J. C. Saez, A. C. Campos De Carvalho, and G. Fishman. 1993. Cardiovascular gap junctions: gating properties, function and dysfunction. In Ion Channels in the Cardiovascular Systems. Academic Press, New York.

Takens-kwak, B. R., and H. J. Jongsma. 1992. Cardiac gap junctions: 3 distinct single channel conductances and their modulation by phosphorylation treatments. Pflügers. Arch. 422:198–200.

Trosko, J. E., C. C. Chang, B. V. Madhukar, and J. E. Klaunig. 1990a. Chemical, oncogene and growth factor inhibition of gap junctional intercellular communication: an integrative hypothesis of carcinogenesis. Pathobiology. 58:265–278.

Trosko, J. E., C. C. Chang, and B. V. Madhukar. 1990b. Symposium: cell communication in normal and uncontrolled growth. Radiat. Res. 123: 241–251.

Tsien, R., and R. Weingart. 1976. Inotropic effect of cyclic AMP in calf ventricular muscle studied by a cut end method. J. Physiol. 260:117–141.

Veenstra, R. D., and R. L. DeHaan. 1986. Measurements of single channel currents from cardic gap junctions. Science. 233:972–974.

Weidmann, S. 1966. The diffusion of radioactive potassium across intercalated disks of mammalian cardiac muscle. J. Physiol. 132:157–163.

Wolfram Research, Inc. 1991. Mathematica. Version 2.0. Wolfram Research, Inc, Champaign, Illinois.

Yamasaki, H., M. Hollstein, M. Mesnil, N. Martel, and A. M. Aguelon. 1987. Selective lack of intercellular communication between transformed and nontransformed cells as a common property of chemical and oncogene transformation of BALB/c3Ts cells. Cancer Res. 47: 5658–5664.